

One-off and Repeating Fast Radio Bursts: A Statistical Analysis

HAO-YAN CHEN,¹ WEI-MIN GU,¹ MOUYUAN SUN,¹ AND TUAN YI¹

¹*Department of Astronomy, Xiamen University, Xiamen, Fujian 361005, P. R. China*

(Received XXX; Revised YYY; Accepted ZZZ)

ABSTRACT

According to the number of detected bursts, fast radio bursts (FRBs) can be classified into two categories, i.e., one-off FRBs and repeating ones. We make a statistical comparison of these two categories based on the first FRB catalog of the Canadian Hydrogen Intensity Mapping Experiment Fast Radio Burst Project. Using the Anderson-Darling, Kolmogorov-Smirnov, and Energy statistic tests, we find significant statistical differences (p -value < 0.001) of the burst properties between the one-off FRBs and the repeating ones. More specifically, after controlling for distance, we find that the peak luminosities of one-off FRBs are, on average, higher than the repeating ones; the pulse temporal widths of repeating FRBs are, on average, longer than the one-off ones. The differences indicate that these two categories could have distinct physical origins. Moreover, we discuss the sub-populations of FRBs and provide statistical evidence to support the existence of sub-populations in one-off FRBs and in repeating ones.

Keywords: High energy astrophysics (739); Radio bursts (1339); Radio transient sources (2008)

1. INTRODUCTION

Fast radio bursts (hereafter FRBs) are extragalactic millisecond-duration radio bursts and have been detected in frequencies from 118 MHz to 8 GHz (e.g., Cordes & Chatterjee 2019; Petroff et al. 2019; Pleunis et al. 2021b). The host galaxies of nineteen FRBs have been identified (Heintz et al. 2020)¹. The origins of FRBs remain mysteries. According to the number of detected bursts, FRBs can be classified into two categories, i.e., repeating FRBs and observational one-off (hereafter one-off) ones. For repeating FRBs, models involve young rapidly rotating pulsars (Lyutikov et al. 2016), a wandering jet in an intermediate-mass black hole (BH) binary with chaotic accretion (Katz 2017), a pulsar passes through the asteroid belt (Dai et al. 2016; Dai & Zhong 2020), a neutron star (NS)-white dwarf (WD) binary with strong dipolar magnetic fields (Gu et al. 2016, 2020), the precession of a jet in an NS/BH-WD binary with super-Eddington accretion rate (Chen et al. 2021), and the intermittent collapses of the crust of a strange star (Geng et al. 2021). For one-off FRBs, models often invoke the collapse of a spinning supra-massive NS forming a BH (Zhang 2014), and the merger of a charged Kerr-Newman BH binary (Zhang 2016; Liu et al. 2016). Therefore, we would expect that the repeating FRBs and one-off ones have different temporal and spectral properties (e.g., CHIME/FRB Collaboration et al. 2019; Fonseca et al. 2020).

Recently, the Canadian Hydrogen Intensity Mapping Experiment Fast Radio Burst (hereafter CHIME/FRB) Project released the first CHIME/FRB catalog (hereafter Catalog 1); the catalog consists of FRBs that were detected between 400 and 800 MHz and from July 25, 2018, to July 1, 2019, (Amiri et al. 2021). Catalog 1 contains 492 unique sources, i.e., 474 one-off FRBs and 18 repeaters². With the same search pipeline, the burst properties can be measured with uniform selection effects. Therefore, this sample is ideal for exploring the statistical properties of FRBs.

Some studies aim to explore the possible differences between one-off FRBs and repeating ones based on Catalog 1. For example, Josephy et al. (2021) studied the Galactic latitudes of one-off FRBs and repeating ones and found that the

¹ <http://frbhosts.org>

² <https://www.chime-frb.ca/catalog>

distribution of FRBs is isotropic. Meanwhile, Amiri et al. (2021) found that the distributions of dispersion measures (DMs) and extragalactic DMs (DM_E) of one-off FRBs and the first-detected repeater events are statistically consistent with originating from the same underlying sample. For the distribution of fluences, Amiri et al. (2021) showed that one-off FRBs and repeaters are statistically similar. On the other hand, Amiri et al. (2021) found that two distinct FRB populations could be inferred from the distribution of the peak fluxes. Moreover, Pleunis et al. (2021a) showed that the “downward-drifting” of frequency and multiple spectral-temporal components, which are absent in one-off FRBs, seem to be common in repeaters. Compared to the distributions of pulse temporal widths and spectral bandwidths, Pleunis et al. (2021a) showed that the repeating FRBs (for the first-detected events) have larger temporal widths and narrower bandwidths than that of one-off ones. Zhong et al. (2022) showed that the distribution distinctions for one-off FRBs and repeaters in the spectral index and the peak frequency cannot be explained by the selection effect due to a beamed emission. These differences all indicate that FRBs might have different populations.

Amiri et al. (2021) only compared 205 one-off FRBs and 18 the first-detected repeater events to explore the differences between the two types of FRBs. The differences in the physical mechanisms of the burst features between repeaters and one-off FRBs could not be found only by analyzing the first-detected repeater events. Moreover, some burst parameters used in Pleunis et al. (2021a), e.g., spectral bandwidth, might be inappropriate to compare the one-off FRBs with the repeating ones. The reason is that, due to the limited instrumental bandwidth, the spectral bandwidth reported in Catalog 1 might be significantly biased and is not an excellent tracer of the FRB intrinsic bandwidth. In addition, some previous works (e.g., Cui et al. 2021; Zhong et al. 2022) did not control for distance when comparing the peak luminosity and energy distributions of the two types of FRBs. Thus, the distinctions of comparisons might be biased. In this work, we demonstrate that one-off FRBs and repeating ones should be two physically distinct populations based on Catalog 1, by investigating several different burst parameters with similar distances, i.e., the fluxes, the pulse temporal widths, and the estimated isotropic peak luminosity L_p .

The remainder of this manuscript is organized as follows. In Section 2, we calculate the peak luminosities of one-off FRBs and repeating ones, and build up the mock samples for repeaters and the control samples for one-off FRBs with matched DM_E to present the differences between the two types of FRBs. In Section 3, we demonstrate statistically that FRBs could be divided into two categories, i.e., one-off FRBs and repeaters. Then, we further discuss whether one-off FRBs and repeaters have sub-populations. Conclusions and discussion are presented in Section 4.

2. THE SAMPLES

Our study utilizes the largest FRB sample to date (i.e., Catalog 1). Catalog 1 consists of 474 one-off FRBs and 18 repeating FRBs (62 bursts). We exclude six one-off sources that have bad gains (Amiri et al. 2021). Thus our sample contains 468 one-off sources plus 18 repeating sources.

2.1. Isotropic Peak Luminosity

To estimate the FRB isotropic peak luminosity (denoted as L_p), we use FRB DMs to estimate their redshifts z and luminosity distances D_L since only three host galaxies of FRBs in Catalog 1 (i.e., FRBs 20121102A, 20180916B, and 20181030A) have been identified (e.g., Zhang 2018; Macquart et al. 2020). The methodology is as follows.

The extragalactic dispersion measure DM_E of an FRB, which takes away the contributions from our Galactic interstellar medium (ISM) ($DM_{MW,ISM}$) based on the Galactic electron density model NE2001 (Cordes & Lazio 2002) or YMW16 (Yao et al. 2017) and halo ($DM_{MW,halo}$), where $DM_{MW,halo} \approx 50 \text{ pc cm}^{-3}$ (Macquart et al. 2020), can be written as

$$DM_E = DM_{IGM} + DM_{\text{host}} , \quad (1)$$

where DM_{IGM} is the contribution from the intergalactic medium (IGM), and DM_{host} is the contribution from the host galaxy of FRB. Amiri et al. (2021) mainly compared the distribution of DM_E based on the NE2001 model. Thus, we only consider the NE2001 model. The DM_{host} can be estimated as $DM_{\text{host}} = 50/(1+z) \text{ pc cm}^{-3}$ (Macquart et al. 2020). The contribution from IGM is roughly proportional to the redshift z of the source through (Deng & Zhang 2014)

$$DM_{IGM} = \frac{3cH_0\Omega_b f_{IGM}}{8\pi Gm_p} \int_0^z \frac{\chi(z)(1+z)}{[\Omega_m(1+z)^3 + \Omega_\Lambda]^{1/2}} dz , \quad (2)$$

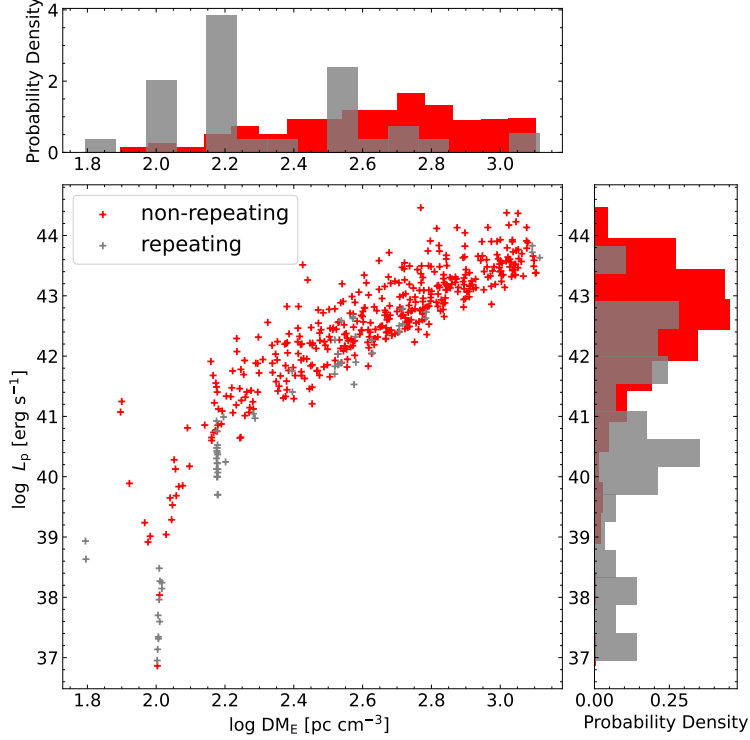


Figure 1. The distributions of DM_E versus L_p for one-off FRBs (red) and repeating FRBs (grey) from Catalog 1. We compare the distributions under the same upper limit of DM_E (or redshifts z). The top and right distributions are marginal probability density estimations of the one-dimensional distribution of the corresponding parameters, i.e., DM_E and L_p . Using the 2DKS test, we can infer the correlation between one-off FRBs and repeaters. There could be evidence that the 2D distributions for one-off FRBs and repeating ones are inconsistent with originating from the same underlying distribution, i.e., $p_{2DKS} \approx 1.18 \times 10^{-10}$. For the E-statistic, the energy distance of ~ 75 ($p_{\text{Energy}} \sim 5 \times 10^{-4}$) confirms the statistical differences between the 2D distributions.

where G is the gravitational constant, f_{IGM} is the fraction of baryons in the IGM with the average value $f_{\text{IGM}} \sim 0.83$ (Fukugita et al. 1998), m_p is the mass of proton, $\chi(z) = (3/4)y_1\chi_{e,H}(z) + (1/8)y_2\chi_{e,He}(z)$ expresses the free electron number per baryon in the universe, $y_1 \sim y_2 \sim 1$ are the hydrogen and helium mass fractions normalized to 3/4 and 1/4, respectively, and $\chi_{e,H}$ and $\chi_{e,He}$ are the ionization fractions for hydrogen and helium, respectively. For FRBs at $z < 3$, both hydrogen and helium are fully ionized (e.g., Yang & Zhang 2016). Thus, $\chi_{e,H} = \chi_{e,He} = 1$ and $\chi(z) \simeq 7/8$. The values of cosmological parameters are adopted from the latest Planck results (Planck Collaboration et al. 2016), i.e., the Hubble constant $H_0 \simeq 67.74 \text{ km s}^{-1} \text{ Mpc}^{-1}$, $\Omega_b \simeq 0.0486$, $\Omega_m \simeq 0.3089$, and $\Omega_\Lambda \simeq 0.6911$. Based on the result of Zhang (2018), the DM_{IGM} can be roughly estimated when $z < 3$

$$DM_{\text{IGM}} \sim z \, 855 \text{ pc cm}^{-3}. \quad (3)$$

In summary, we can use Equations (1)-(3) to estimate DM_{IGM} and redshift z (and the corresponding luminosity distance D_L).

The isotropic peak luminosity L_p of each one-off FRB or every burst of each repeating one is (Zhang 2018)

$$L_p \simeq 4\pi \left(\frac{D_L}{10^{28} \text{ cm}} \right)^2 \left(\frac{S_\nu}{\text{Jy}} \right) \left(\frac{\nu_c}{\text{GHz}} \right) \times 10^{42} \text{ erg s}^{-1}, \quad (4)$$

where S_ν is the observed peak flux density of an FRB, and ν_c is the central frequency of the telescope, i.e., for CHIME, $\nu_c = 600 \text{ MHz}$.

We present in Figure 1, the distributions of DM_E and L_p (and their joint distribution) for one-off FRBs (red) and repeating ones (grey). We compare the distributions of DM_E and L_p under the same upper limit of DM_E . The peaks of the DM_E and L_p distributions of repeaters tend to be smaller and lower than that of one-off ones, respectively. Using

the two-dimensional Kolmogorov-Smirnov (2DKS) test³ (Peacock 1983; Fasano & Franceschini 1987), we compare the joint distribution of DM_E and L_p for one-off FRBs with that for repeating ones; we find that the differences between the two joint distributions are statistically significant since the corresponding p_{2DKS} -value is $\sim 1.18 \times 10^{-10}$. In addition to the 2DKS test, we use the Energy statistic⁴ (E-statistic; e.g., Gábor & Maria 2013) for two-dimensional data to verify the differences in the two joint distributions of one-off FRBs and repeating ones. The E-statistic test compares the energy distance between the distributions of the different samples. The energy distance is zero if and only if the distributions are identical. The energy distance of two joint distributions for one-off FRBs and repeating ones is ~ 75 ($p_{\text{Energy}} \sim 5 \times 10^{-4}$), implying that the two joint distributions of DM_E and L_p are significantly different. The observed differences suffer from strong statistical biases, since the two types of FRBs have different DM_E distributions. Below, we explore this point in detail.

2.2. The Mock Samples

As shown in Figure 1, one-off FRBs and repeating ones have different distributions of L_p . The differences might be intrinsic, i.e., one-off FRBs and repeaters have distinct bursting energy generation mechanisms, or caused by the differences in redshift z (or D_L). Hence, we perform the following Monte Carlo experiment to build the mock samples of repeaters and one-off FRBs with the matched DM_E to verify whether the differences are intrinsic. Unlike previous works, which only chose the physical properties of the first-detected burst for each repeater to explore the differences between the two types of FRBs (e.g., Amiri et al. 2021; Pleunis et al. 2021a), we consider each repeating burst as an independent mock FRB source. The reason is that, as shown in Figure 1, the peak luminosities of different bursts from the same repeater vary greatly (e.g., ~ 1.5 magnitudes for FRB 20180916B). The burst features of the repeaters could not be revealed only by analyzing the first-detected bursts. We expect that, if the physical mechanisms for one-off FRBs and repeating ones are the same, the peak luminosity distribution of all bursts in repeating FRBs is statistically similar to bursts in one-off ones after controlling DM_E . We conduct Monte Carlo experiments to test the expectation. In the Monte Carlo experiments, we need to ensure that each burst of repeaters has a corresponding one-off FRB with a similar DM_E , i.e., $|DM_{\text{repeating}} - DM_{\text{one-off}}|/DM_{\text{repeating}} \lesssim 0.05$. For the repeaters, the minimum value of the DM_E is 62.5 pc cm^{-3} of FRB 20181030A. None of the one-off FRBs has the similar DM_E as FRB 20181030A since the minimum value of the one-off FRB DM_E is 78.8 pc cm^{-3} . Thus, for the Monte Carlo experiments, we reject the repeater FRB 20181030A and consider the remaining 17 repeaters which have a total number of 60 bursts.

The steps to conduct the Monte Carlo experiments are as follows. First, we randomly select (with replacement) 60 mock repeating FRBs from the 17 repeaters. Hence, each repeater can be selected multiple times (n_r), and the statistical expectation of n_r is the same for all repeaters. Second, for each mock repeating FRB, we randomly select (with replacement) one burst, whose DM is the same as the mock repeating FRB. That is, we eventually obtain 60 bursts (hereafter repeating mock sample) from the repeating FRBs, and the contribution of each repeater to the mock sample is statistically the same. The DM distribution of the repeating mock sample is different from that of the original 60 bursts mentioned in Section 2.1 and Figure 1, but resembles the DM distribution of the 17 repeaters. Third, for each repeating mock burst, we randomly select a one-off FRB with the similar DM_E (hereafter the one-off control sample). Hence, the repeating mock sample and the one-off control sample share identical DM_E distributions (see the left panel of Figure 2). Then, we compare the peak luminosity distributions of the repeating mock sample and the one-off control sample (see the right panel of Figure 2). We repeat this experiment ten thousand times. The mean distributions (and their 2σ uncertainties) of the peak luminosities L_p of bursts from the repeating mock samples and one-off control samples are calculated.

We use the Kolmogorov-Smirnov (KS) test to assess whether there are statistical differences between the repeating mock samples and the one-off control samples. The two samples are statistically different if the p -values of the KS tests are smaller than 5%. The probability density distributions of the DM_E and L_p for a realization of the repeating mock and the one-off control samples are shown in Figure 2. For the distributions of DM_E (the left panel of Figure 2), the p -value of the KS test is ~ 0.95 . For the distributions of L_p (the right panel of Figure 2), the p -value of the K-S test is $\sim 4.16 \times 10^{-6}$, indicating that two mock samples could originate from different underlying peak-luminosity distributions after controlling for DM_E . For the ten thousand simulations, while the p -value of the K-S test for the DM_E distributions (the left panel of Figure 3) is always larger than 0.05, the p -value for the L_p distributions (the right

³ <https://github.com/syrte/ndtest/blob/master/ndtest.py>

⁴ The E-statistic can be available for R on the Comprehensive R Archive Network (CRAN) under general public license, i.e., *energy* package (<https://cran.r-project.org/web/packages/energy/index.html>).

panel of Figure 3) is smaller than 0.05 in 90% of simulations. We also use the E-statistic test to check the statistical differences in the distributions of DM_E and L_p and obtain the same conclusions.

Some studies have found the differences in the temporal widths between repeating FRBs and one-off ones (e.g., Amiri et al. 2021; Pleunis et al. 2021a). Therefore, in addition to the comparison of the luminosity distributions, we follow the above procedures to compare the distributions of the pulse temporal widths of repeating FRBs and one-off ones. The mean distributions and the corresponding 2σ statistical uncertainties are evaluated. In our comparisons, after controlling for DM_E , the pulse temporal widths of two types of FRBs would have similar dispersive delays (e.g., Equation (4) in Petroff et al. 2019), which could help to compare the distribution distinctions for the intrinsic pulse temporal widths between one-off FRBs and repeaters. For the peak flux density S_ν , there is a correlation between L_p and S_ν (see Equation (4)). Hence, we mainly compare the differences in L_p and the burst temporal widths between repeating FRBs and one-off ones. For the distributions of the temporal widths, there are statistical differences between the repeating mock samples and the one-off control samples since the p -values of the KS and E-statistic tests are always less than 0.001 in all simulations.

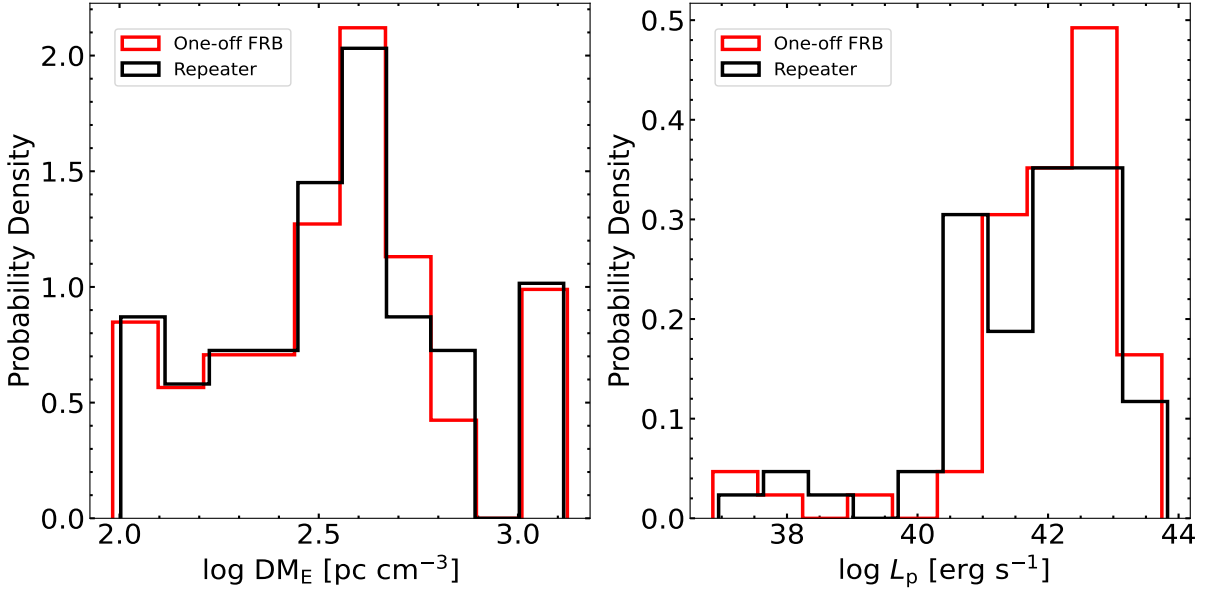


Figure 2. The probability density distributions of DM_E (the left panel) and L_p (the right panel) for a random realization of the repeating mock and the one-off control samples. For the distribution of DM_E , two samples should arise from the same group, i.e., $p_{KS} \approx 0.95$. For the distribution of L_p , two mock samples could originate from different underlying distributions, since $p_{KS} \approx 4.16 \times 10^{-6}$.

3. THE POPULATIONS OF FRBS

3.1. Repeating and one-off FRBs

Figure 4 shows the mean distributions of L_p (the left panel) and the pulse temporal widths (the right panel) for the bursts of repeating FRBs and one-off ones with similar DM_E . Their corresponding 2σ statistical uncertainties are shown as the shaded regions. We use the Anderson-Darling (AD) and KS tests to assess the statistical differences in two FRB samples in terms of L_p and the temporal width. The null hypotheses of the AD and KS tests are that the two samples are drawn from the same population. If the p -values of the AD and KS tests are smaller than 5%, we reject the null hypothesis and conclude that the two samples are statistically different. For the distributions of L_p (the left panel of Figure 4), we find that the p -values of KS and AD tests are less than 0.001. That is, the bursts of the two FRB samples have intrinsically different luminosity distributions (the mean L_p for repeaters is $\log(L_{re}/\text{erg s}^{-1}) \simeq 40.14 \pm 0.71$; for one-off FRBs is $\log(L_{one}/\text{erg s}^{-1}) \simeq 41.41 \pm 0.65$) and the difference is more evident at the low luminosity end ($\log(L_{re}/\text{erg s}^{-1}) \lesssim 39$). Moreover, for the distributions of temporal widths (the right panel of Figure 4), we find that the p -values of KS and AD tests are smaller than 0.001. That is, the bursts of the two FRB samples have distinct distributions of the temporal width (the mean temporal width for repeaters is

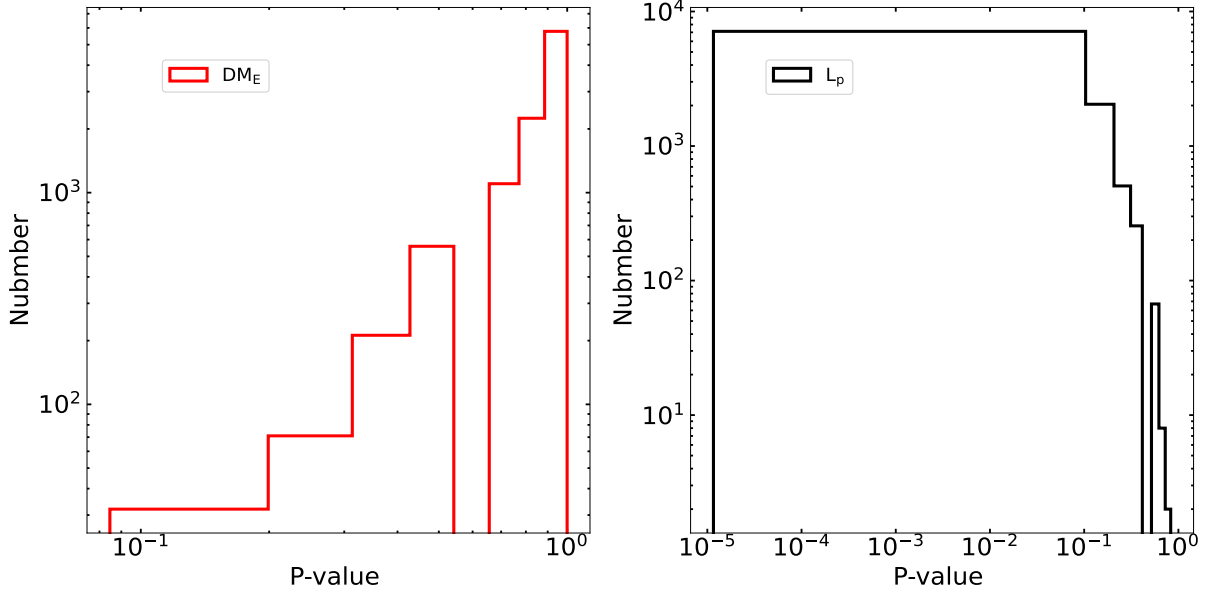


Figure 3. Left: the p -value of the K-S test for the DM_E distributions of the two mock samples in the ten thousand simulations. Right: the same as the left panel, but for L_p . For all simulations, the p -value for DM_E is always larger than 0.05. For 90% of simulations, the p -value for L_p is smaller than 0.05.

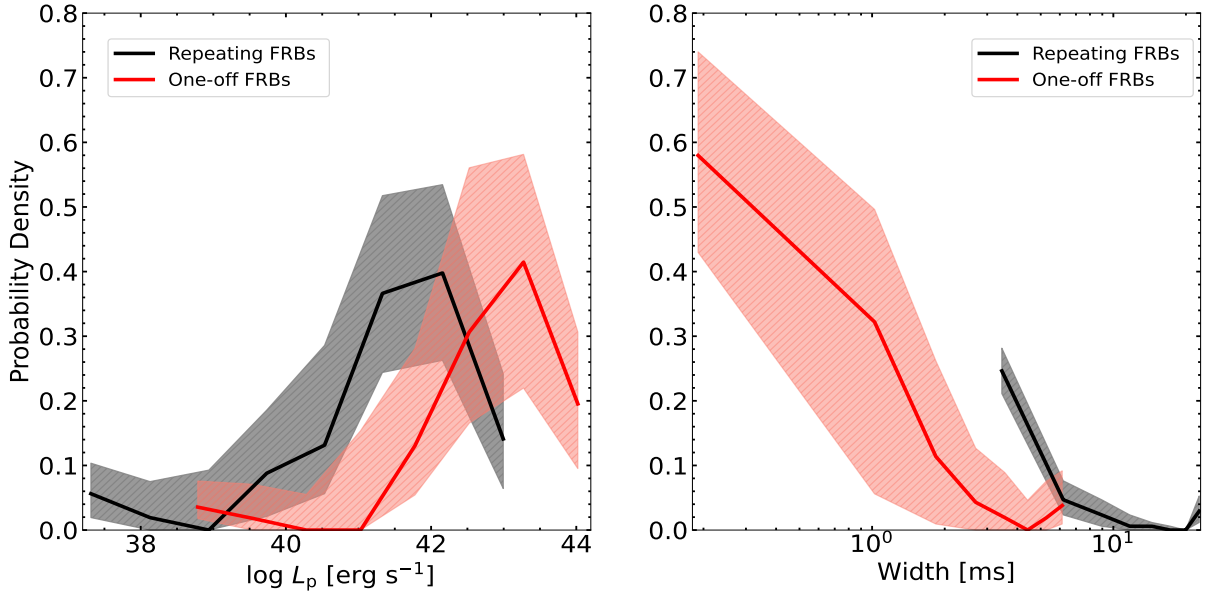


Figure 4. The probability density distributions of L_p (left) and intrinsic temporal widths (right) for one-off FRBs and repeating ones. In both panels, the red lines show the mean distributions of one-off control samples and the black lines represent the mean distributions of repeating mock samples. All shadow areas indicate the two-sigma (95%) confidence intervals. The distributions of L_p show that the peak luminosities of one-off sources are, on average, higher than the repeating ones. The distributions are inconsistent with arising from the same FRB group (i.e., $p_{AD} < 0.001$, $p_{KS} \approx 2 \times 10^{-6}$). Furthermore, as shown by the distributions of temporal widths, the pulse temporal widths of repeating FRBs are, on average, longer than the one-off ones. There is evidence that two FRB populations might originate from different underlying distributions, i.e., $p_{AD} < 0.001$ and $p_{KS} \approx 2.5 \times 10^{-5}$.

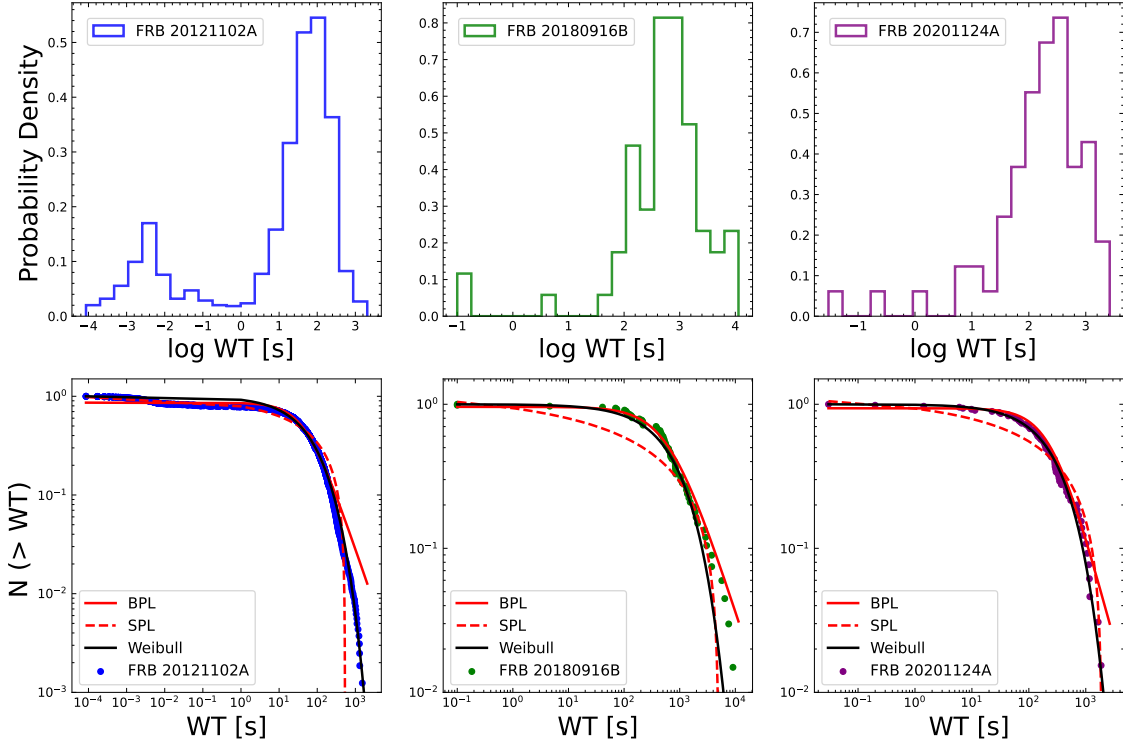


Figure 5. Top: the distributions of waiting times (WTs) of three active repeating FRBs. The WT distributions of FRB 20121102A show a bimodal structure, whereas other FRBs, i.e., FRBs 20180916B and 20201124A, have unimodal structures. Bottom: the cumulative distribution functions (CDFs) of WTs of three FRBs. Three distribution models, i.e., the bent power law (BPL; red line), the simple power law (SPL; dashed red line), and Weibull model (black line), are considered to fit the CDFs of WT. The data for FRB 20121102A is taken from Li et al. (2021); the data for FRB 20180916B is taken from Chawla et al. (2020), CHIME/FRB Collaboration et al. (2020), Marthi et al. (2020), Pastor-Marazuela et al. (2021), and Pleunis et al. (2021b); the data for FRB 20201124A is taken from Hilmansson et al. (2021), and Marthi et al. (2022).

13.08 ± 2.38 ms; for one-off ones is 3.14 ± 0.74 ms) and the difference is more evident at the long temporal width end ($\gtrsim 7$ ms). These differences support the speculation that the emission mechanisms of the bursts in the two types of FRBs should be distinct.

3.2. Sub-populations

As mentioned in Section 3.1, repeating FRBs and one-off ones should have distinct emission mechanisms. Do one-off FRBs and repeating FRBs have sub-populations?

For one-off FRBs, the single-pulse bursts are commonly detected (e.g., CHIME/FRB Collaboration et al. 2019), whereas CHIME/FRB Collaboration et al. (2021) detected the multi-component pulse profiles of three one-off FRBs, i.e., FRBs 20191221A, 20210206A, and 20210213A, and identified the periodic separations of these components. The complex and periodic profiles indicate that there could exist a sub-group of one-off FRBs which have similar physical processes or host environments to some repeaters.

For periodicity, two repeating sources have been found periodic activities, i.e., FRBs 20180916B (16.35-day activity period; see CHIME/FRB Collaboration et al. 2020) and 20121102A (~ 157 -day activity period; see Cruces et al. 2021). Some repeaters with more than 20 bursts recorded by CHIME were not found to have any periodic activity, e.g., FRBs 20180814A (22 bursts), 20190303A (27 bursts), and 20201124A (34 bursts). The differences in periodicity of repeating FRBs might indicate that the repeaters could have different groups, i.e., the periodic repeaters and the aperiodic repeaters (e.g., Katz 2017; Lin et al. 2022).

For active repeaters, we can study the waiting time (WTs) distributions to understand the physical mechanism of repeating FRBs (e.g., Wang & Yu 2017; Zhang et al. 2021). The WTs are the time intervals between two adjacent (detected) bursts measured during periods of continuous observation. Up till now, the most active repeaters are FRBs 20121102A (e.g., Li et al. 2021), 20180916B (e.g., CHIME/FRB Collaboration et al. 2020) and 20201124A (e.g., Xu et

al. 2021). As shown in the top three panels of Figure 5, the distributions of WTs for three active repeating FRBs have different features. i.e., a bimodal structure for FRB 20121102A, and unimodal structures for FRBs 20180916B and 20201124A. We can infer some progenitor models for repeaters from the cumulative distributions functions (CDFs) of WTs. Three models are proposed to fit the CDFs of WTs, i.e., simple power law (SPL) (e.g., the soft gamma repeaters (SGRs)-like model for FRB 121102; Wang & Yu 2017), bent power law (BPL) (e.g., SGR J1550-5418; Chang et al. 2017), and Weibull function (e.g., Oppermann et al. 2018). The SPL model is expressed as (Sang & Lin 2021)

$$N(> \delta t) = A (\delta t^{-\alpha} - t_c^{-\alpha}) , \quad (5)$$

where δt is the waiting time and t_c is the cut-off value with $N(> t_c) = 0$. The BPL model is taken the form (Sang & Lin 2021)

$$N(> \delta t) = B \left[1 + \left(\frac{\delta t}{t_m} \right)^\beta \right]^{-1} , \quad (6)$$

where t_m is the median value, i.e., the number of bursts with $\delta t > t_m$ is equal to the number of bursts with $\delta t < t_m$. The Weibull function is described as (e.g., Oppermann et al. 2018)

$$N(> \delta t) = e^{-(\delta t r \Gamma(1+1/k))^k} , \quad (7)$$

where k is the shape parameter, r is the event rate, and Γ is the gamma function. The Weibull distribution is equivalent to a Poisson distribution when $k = 1$, while $k \sim 1$ implies that the bursts are clustered, with more clustering implied for lower k . The fitting results are shown in the bottom three panels of Figure 5. The best-fitting parameters and their 1σ uncertainties for three fitting models are shown in Table 1. The χ^2 , defined as $\chi^2 = \sum [(N_i - N_{i,\text{model}})^2 / N_i]$, where N_i and $N_{i,\text{model}}$ are the data of the WT distributions and the fitting models, respectively, can be used to evaluate the goodness of fit of the fitting models for the CDFs of WTs. The minimum value of χ^2 corresponds to the best-fitting models. We find that the CDFs of WTs for FRBs 20121102A and 20201124A can be well fitted by the Weibull function; the WT distribution of FRB 20180916B is well fitted by the BPL model. That is, the central engine of these active repeating FRBs could be magnetars, while the physical mechanisms should be distinct. Using the KS test (and the AD test), we compare the correlations of the distributions of WTs for three active repeating FRBs. There is evidence that three active repeaters should come from different groups, i.e., for FRBs 20121102A and 20180916B, $p_{\text{KS}} = 0$; for FRBs 20121102A and 20201124A, $p_{\text{KS}} \approx 1.67 \times 10^{-10}$; for FRBs 20180916B and 20201124A, $p_{\text{KS}} \approx 7.77 \times 10^{-16}$.

Table 1. The best-fitting parameters for three CDF models

FRB	SPL			BPL			Weibull		
	α	t_c (s)	χ^2	β	t_m (s)	χ^2	r (day $^{-1}$)	k	χ^2
FRB 20121102A	$-0.25^{+0.05}_{-0.05}$	$534.91^{+200.67}_{-122.19}$	416.85	$1.14^{+0.29}_{-0.24}$	$51.54^{+11.40}_{-9.84}$	8.99	$864.25^{+59.23}_{-43.13}$	$0.59^{+0.12}_{-0.11}$	7.94
FRB 20180916B	$-0.16^{+0.05}_{-0.09}$	$5060.89^{+1832.79}_{-1936.96}$	4.86	$1.21^{+0.53}_{-0.58}$	$684.99^{+214.72}_{-252.55}$	0.34	$86.43^{+25.56}_{-21.84}$	$0.78^{+0.18}_{-0.15}$	0.39
FRB 20201124A	$-0.22^{+0.06}_{-0.10}$	$1926.37^{+716.62}_{-626.42}$	1.28	$1.48^{+0.34}_{-0.33}$	$264.05^{+142.98}_{-105.77}$	0.52	$241.92^{+83.68}_{-75.04}$	$0.83^{+0.11}_{-0.10}$	0.14

In addition to comparing differences in the CDFs of WTs, we would like to compare the differences between the active repeating FRBs in the joint distributions of L_p and WTs. As shown in Figure 6, ΔL_p represents the luminosity differences between two adjacent (detected) bursts, i.e., $\Delta L_p = \log(L_{p,i+1}) - \log(L_{p,i})$, where $L_{p,i}$ represents the peak luminosity of the i -th burst. We use the E-statistic test to verify the differences in the joint distributions of three active repeaters in terms of WTs and ΔL_p . There is significant evidence that three active repeaters should originate from distinct populations, i.e., for FRBs 20121102A and 20180916B, the energy distance of ~ 26128 ($p_{\text{Energy}} \sim 1 \times 10^{-4}$); for FRBs 20121102A and 20201124A, the energy distance of ~ 8562 ($p_{\text{Energy}} \sim 7 \times 10^{-4}$); for FRBs 20180916B and 20201124A, the energy distance of ~ 5719 ($p_{\text{Energy}} \sim 5 \times 10^{-4}$).

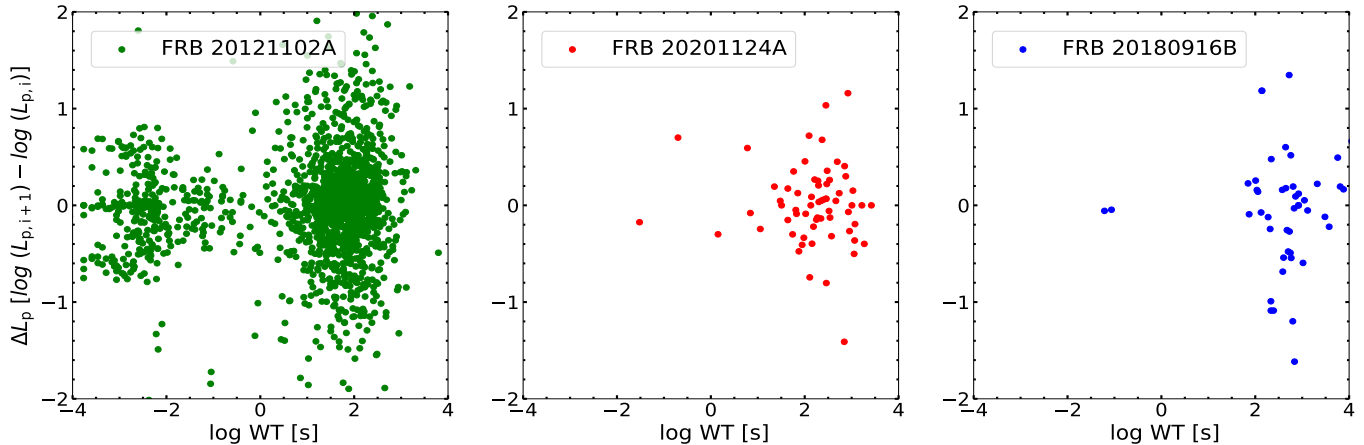


Figure 6. The joint distributions of the WTs and the luminosity differences $\Delta L_p = \log(L_{p,i+1}) - \log(L_{p,i})$. Three active repeaters should originate from distinct groups, i.e., for FRBs 20121102A and 20180916B, the energy distance of ~ 26128 ($p_{\text{Energy}} \sim 1 \times 10^{-4}$); for FRBs 20121102A and 20201124A, the energy distance of ~ 8562 ($p_{\text{Energy}} \sim 7 \times 10^{-4}$); for FRBs 20180916B and 20201124A, the energy distance of ~ 5719 ($p_{\text{Energy}} \sim 5 \times 10^{-4}$).

Moreover, the polarization of repeating FRBs is also a significant feature that suggests the diversity of repeaters. FRB 20121102A was found to be $\sim 100\%$ linearly polarized and had the rotation measure (RM) about $\sim 10^5$ rad m^{-2} , which implies an extreme magneto-ionic environment (e.g., Michilli et al. 2018). FRB 20180916B was also found to be $\sim 100\%$ linearly polarized yet is not surrounded by a dense supernova remnant since $|\text{RM}| \sim 10^2$ rad m^{-2} (Pastor-Marazuela et al. 2021). In addition, some bursts of FRB 20201124A showed the signs of circular polarization, which were first found in repeating FRBs (e.g., Hilmarsson et al. 2021). The discrepancies of the distributions of WTs and the polarization characteristics suggest that the central engine of repeating FRBs could be magnetars, while the emission mechanisms (e.g., pulsar-like or GRB-like mechanisms; see the review of Zhang 2020) and host environments (e.g., the magnetic field strengths; Zhong et al. 2022) should be distinct.

4. CONCLUSIONS AND DISCUSSION

In this paper, we have statistically studied the differences in the burst properties between one-off FRBs and repeaters in Catalog 1. We found that one-off FRBs and repeating ones have different burst L_p and temporal width distributions, indicating that the two samples have distinct physical origins (see Figure 4; Section 3.1). Moreover, we discuss the sub-populations of one-off FRBs and repeating ones and provide a piece of evidence to support the existence of sub-populations in both types of FRBs (see Figures 5 and 6; Section 3.2).

Our work can be advanced in terms of the sample size. Chen et al. (2022) used unsupervised machine learning to classify repeaters and one-off FRBs from Catalog 1 and identified 188 repeating FRB candidates from 474 one-off sources, suggesting a large fraction of repeating FRBs could be missed due to the lack of monitoring observations. Recently, Li et al. (2021) detected 1652 independent burst events from FRB 20121102A by FAST. The flux limit of this sample is at least three times lower than those of previously observed samples for FRB 20121102A. Therefore, the sensitive radio telescopes, e.g., FAST, can detect many faint bursts to help to reveal the physical nature of FRBs and to determine whether the distinct populations of FRBs are present.

ACKNOWLEDGMENTS

We thank the scientific and statistic referees for helpful comments that significantly improved the paper. This work was supported by the National Key R&D Program of China under grant 2021YFA1600401, and the National Natural Science Foundation of China under grants 11925301, 11973002, 12033006, and 12221003.

REFERENCES

- Amiri, M., Andersen, B. C., Bandura, K., et al. 2021, ApJS, 257, 59. doi:10.3847/1538-4365/ac33ab
- Chang, Z., Lin, H.-N., Sang, Y., et al. 2017, Chinese Physics C, 41, 065104. doi:10.1088/1674-1137/41/6/065104

- Chawla, P., Andersen, B. C., Bhardwaj, M., et al. 2020, *ApJL*, 896, L41. doi:10.3847/2041-8213/ab96bf
- Chen, B. H., Hashimoto, T., Goto, T., et al. 2022, *MNRAS*, 509, 1227. doi:10.1093/mnras/stab2994
- Chen, H.-Y., Gu, W.-M., Sun, M., et al. 2021, *ApJ*, 921, 147. doi:10.3847/1538-4357/ac1fe9
- CHIME/FRB Collaboration, Andersen, B. C., Bandura, K., et al. 2019, *ApJL*, 885, L24. doi:10.3847/2041-8213/ab4a80
- CHIME/FRB Collaboration, Amiri, M., Andersen, B. C., et al. , *Nature*, 582, 351. doi:10.1038/s41586-020-2398-2
- CHIME/FRB Collaboration, Andersen, B. C., Bandura, K., et al. 2021, arXiv:2107.08463
- Cordes, J. M. & Chatterjee, S. 2019, *ARA&A*, 57, 417. doi:10.1146/annurev-astro-091918-104501
- Cordes, J. M. & Lazio, T. J. W. 2002, *astro-ph/0207156*
- Cruces, M., Spitler, L. G., Scholz, P., et al. 2021, *MNRAS*, 500, 448. doi:10.1093/mnras/staa3223
- Cui, X.-H., Zhang, C.-M., Wang, S.-Q., et al. 2021, *MNRAS*, 500, 3275. doi:10.1093/mnras/staa3351
- Dai, Z. G., Wang, J. S., Wu, X. F., et al. 2016, *ApJ*, 829, 27. doi:10.3847/0004-637X/829/1/27
- Dai, Z. G. & Zhong, S. Q. 2020, *ApJL*, 895, L1. doi:10.3847/2041-8213/ab8f2d
- Deng, W. & Zhang, B. 2014, *ApJL*, 783, L35. doi:10.1088/2041-8205/783/2/L35
- Fasano, G. & Franceschini, A. 1987, *MNRAS*, 225, 155. doi:10.1093/mnras/225.1.155
- Fonseca, E., Andersen, B. C., Bhardwaj, M., et al. 2020, *ApJL*, 891, L6. doi:10.3847/2041-8213/ab7208
- Fukugita, M., Hogan, C. J., & Peebles, P. J. E. 1998, *ApJ*, 503, 518. doi:10.1086/306025
- Gabor, J. & Maria, L. 2013, *Journal of Statistical Planning and Inference*, 143, 8. doi:10.1016/j.jspi.2013.03.018
- Geng, J., Li, B., & Huang, Y. 2021, *The Innovation*, 2, 100152. doi:10.1016/j.xinn.2021.100152
- Gu, W.-M., Dong, Y.-Z., Liu, T., et al. 2016, *ApJL*, 823, L28. doi:10.3847/2041-8205/823/2/L28
- Gu, W.-M., Yi, T., & Liu, T. 2020, *MNRAS*, 497, 1543. doi:10.1093/mnras/staa1914
- Heintz, K. E., Prochaska, J. X., Simha, S., et al. 2020, *ApJ*, 903, 152. doi:10.3847/1538-4357/abb6fb
- Hilmarsson, G. H., Spitler, L. G., Main, R. A., et al. 2021, *MNRAS*, 508, 5354. doi:10.1093/mnras/stab2936
- Josephy, A., Chawla, P., Curtin, A. P., et al. 2021, *ApJ*, 923, 2. doi:10.3847/1538-4357/ac33ad
- Katz, J. I. 2017, *MNRAS*, 471, L92. doi:10.1093/mnras/slx113
- Li, D., Wang, P., Zhu, W. W., et al. 2021, *Nature*, 598, 267. doi:10.1038/s41586-021-03878-5
- Lin, Y.-Q., Chen, H.-Y., Gu, W.-M., et al. 2022, *ApJ*, 929, 114. doi:10.3847/1538-4357/ac5c49
- Liu, T., Romero, G. E., Liu, M.-L., et al. 2016, *ApJ*, 826, 82. doi:10.3847/0004-637X/826/1/82
- Lyutikov, M., Burzawa, L., & Popov, S. B. 2016, *MNRAS*, 462, 941. doi:10.1093/mnras/stw1669
- Macquart, J.-P., Prochaska, J. X., McQuinn, M., et al. 2020, *Nature*, 581, 391. doi:10.1038/s41586-020-2300-2
- Marthi, V. R., Gautam, T., Li, D. Z., et al. 2020, *MNRAS*, 499, L16. doi:10.1093/mnras/laaa148
- Marthi, V. R., Bethapudi, S., Main, R. A., et al. 2022, *MNRAS*, 509, 2209. doi:10.1093/mnras/stab3067
- Michilli, D., Seymour, A., Hessels, J. W. T., et al. 2018, *Nature*, 553, 182. doi:10.1038/nature25149
- Oppermann, N., Yu, H.-R., & Pen, U.-L. 2018, *MNRAS*, 475, 5109. doi:10.1093/mnras/sty004
- Pastor-Marazuela, I., Connor, L., van Leeuwen, J., et al. 2021, *Nature*, 596, 505. doi:10.1038/s41586-021-03724-8
- Peacock, J. A. 1983, *MNRAS*, 202, 615. doi:10.1093/mnras/202.3.615
- Petroff, E., Hessels, J. W. T., & Lorimer, D. R. 2019, *A&A Rv*, 27, 4. doi:10.1007/s00159-019-0116-6
- Planck Collaboration, Ade, P. A. R., Aghanim, N., et al. 2016, *A&A*, 594, A13. doi:10.1051/0004-6361/201525830
- Pleunis, Z., Good, D. C., Kaspi, V. M., et al. 2021a, *ApJ*, 923, 1. doi:10.3847/1538-4357/ac33ac
- Pleunis, Z., Michilli, D., Bassa, C. G., et al. 2021b, *ApJL*, 911, L3. doi:10.3847/2041-8213/abec72
- Sang, Y. & Lin, H.-N. 2021, *MNRAS*. doi:10.1093/mnras/stab3600
- Wang, F. Y. & Yu, H. 2017, *JCAP*, 2017, 023. doi:10.1088/1475-7516/2017/03/023
- Xu, H., Niu, J. R., Chen, P., et al. 2021, arXiv:2111.11764
- Yang, Y.-P. & Zhang, B. 2016, *ApJL*, 830, L31. doi:10.3847/2041-8205/830/2/L31
- Yao, J. M., Manchester, R. N., & Wang, N. 2017, *ApJ*, 835, 29. doi:10.3847/1538-4357/835/1/29
- Zhang, B. 2014, *ApJL*, 780, L21. doi:10.1088/2041-8205/780/2/L21
- Zhang, B. 2016, *ApJL*, 827, L31. doi:10.3847/2041-8205/827/2/L31
- Zhang, B. 2018, *ApJL*, 867, L21. doi:10.3847/2041-8213/aae8e3
- Zhang, B. 2020, *Nature*, 587, 45. doi:10.1038/s41586-020-2828-1
- Zhang, G. Q., Wang, P., Wu, Q., et al. 2021, *ApJL*, 920, L23. doi:10.3847/2041-8213/ac2a3b
- Zhong, S.-Q., Xie, W.-J., Deng, C.-M., et al. 2022, arXiv:2202.04422